

The effect of Copper Concentration on the Structural , Morphological and Optical Properties of CdS:Cu Nanocrystalline prepared by chemical bath deposition

Nada K. Abbas¹, Ahlam M. Farhan², Ruqayah A. ulwali¹ and Nagham Y. Ahmed¹

Abstract— Undoped Cadmium sulfide (CdS) nanocrystalline thin film and doped copper are prepared by chemical bath deposition (CBD) technique onto glass substrates at ($80 \pm 2^\circ\text{C}$), with average thickness of about (300 nm) have been investigated. The characterization of the product was done by UV-VIS absorption, x-ray diffraction (XRD) and atomic force microscopy (AFM) . The effect of copper content on structural, morphological and several optical properties have been studied. The X-ray diffraction (XRD) analysis revealed that the films were polycrystalline with hexagonal structure and preferential orientation along (002) and exhibited two phases; cubic and hexagonal structure . Atomic force microscopy images show uniform, homogeneous and strong adherent to undoped (CdS) nanocrystalline and doped Copper over the entire glass substrate surface without any voids, pinholes or cracks . This reveals a continuous granular morphology for the films and the band gap of the thin films which are found to be direct allowed transition . The result also shows that the absorption coefficient, extinction coefficient, real and imaginary parts of dielectric constant are tending to increase with the increasing of Cu concentration.

Keywords– nanocrystalline CdS , chemical bath deposition, Cu concentration, the characterization of (CdS:Cu) :absorption, x-ray diffraction and atomic force microscopy.

1 Introduction

Ultrathin semiconductor nanocrystalline thin films have attracted growing interest for both fundamental research and technical application due to their size-dependent electronic properties that has led to a wide range of technological applications as functional layers in electronic and optoelectronic devices, solar cells, photoelectrodes, photocatalysts, and sensors [1]. Nanocrystalline binary and ternary semiconductors of Groups II-VI have potential applications in many technical fields, including photoluminescence, solar cells and photovoltaic applications [2-3].

CdS films nano particles can be processed utilizing various methods and chemical bath deposition is one successful method.

- Prof. Nada Khair Abbas, Ph.D. in the Department of Physics, *College of Science for women*, University of Baghdad .Iraq **E-mail:** nadabbs@yahoo.com
- Prof. Dr. Ahlam M. Farhan : Ph.D. in the Department of Chemistry, *College of Science for women*, University of Baghdad .Iraq **E-mail:** ahlam63a@yahoo.com

Deposition of CdS using CBD is based on the gradual release of Cd^{2+} ions and S^{2-} ions in aqueous alkali bath and the subsequent condensation of these ions on substrate suitably mounted in the bath.

The progressive release of Cd^{2+} ions is achieved by adding a complexing agent (ligand) to the Cd salt to form some cadmium complex species which upon dissociation, results in the release of small concentrations of Cd^{2+} ions. The S^{2-} ions are supplied by decomposition of thiourea [4].

It is important to study the physical properties of particles with diameters between 1 and 100 nm which markedly differ from those of the corresponding bulk materials [5], the UV/V is a spectra for CdS nanoparticles different from the spectrum of bulk CdS [6].

Bulk CdS has direct band gap of 2.4 eV, which falls in the visible spectrum at room temperature [7]. CdS exist in two phases; hexagonal with $a=4.1370 \text{ \AA}$ and $c=6.7144 \text{ \AA}$ [8] and cubic with $a=5.8330 \text{ \AA}$ [9], the hexagonal (wurtzite) CdS films are preferable for solar cell applications due to their excellent stability in photoelectric conversion and heterogeneous photocatalysis. However, challenging to obtain the film from a hexagonal structure only [10] .

Foreign atoms or impurity atoms, may be present in a crystal lattice to improve or change certain semiconductor properties. Impurity atoms may be located at normal lattice sites, in which case they are called substitutional impurities. Impurity atoms may also be located between normal sites, as they are labeled as interstitial impurities. Some impurities, such as oxygen in silicon, tend to be essentially inert; however, other impurities, such as gold or phosphorus in silicon, can drastically alter the properties of the material.[11]

Several techniques were employed for the growth of the ternary CdSCu films. The study analyses CdS:Cunanocrystalline which were deposited by Chemical Bath Deposition(CBD) technique at different composition of (molar concentrations) and to study the effect of copper concentration on the structural, morphological and optical properties of these films. This study aims to discuss the importance of window layer of solar cells and other application .

2 EXPERIMENTAL PROCEDURE

The CdS:Cu thin films were prepared utilizing CBD technique on commercial glass slide for various copper concentration (0,1,2,3and ,4)% . Initially, materials which were used are $\text{CdCl}_2 \cdot \text{H}_2\text{O}$ (0.1M) as Cd^{2+} ion source, CuCl_2 (1,2,3,4)% as Cu^{2+} ion source, thiourea (0.1M) as an S^{2-} ion source and ammonia was used as a complexing agent to control the Cd^{2+} and Cu^{2+} ion concentrations .CdS: Cu nanocrystalline(M = 0, 0.01, 0.02, 0.03 and 0.04) were prepared using an aqueous solution through chemical precipitation technique starting from (1-M)*0.1M CdCl_2 , (M)*0.1 M CuCl_2 , 0.1M thiourea (to provide sulfur), and ammonia which is used as a complexing agent and to adjust the pH at (10.5-11) (using PH-meter model HANNA pHep211). The clean substrates are immersed vertically in the bath beaker for about 40 min .An alkaline solution of ammonia was used to adjust pH of the reaction mixture .The process involves a controllable chemical reaction at a low rate, by adjusting the pH value and temperature of the working solution allows maintaining the stoichiometry constant for any ratio of anions and cations . The temperature of chemical bath was adjusted with hot plate and temperature controller ($80 \pm 2^\circ\text{C}$) , while magnetic stirrer is applied to

promote ion-by-ion heterogeneous growth on the substrate . The pH value of working solution was adjusted using a pH meter and is kept in between 10.5 and 11 for different deposition time (10-40min.). After deposition of the substrates were removed from the chemical bath and cleaned in distilled water.

The films were characterized by X-ray diffraction technique using (Philips X-ray diffractometer) with $\text{CuK}\alpha$ radiation with wavelength $(1.5406)\text{\AA}$. A(UV-160A UV-visible recording) spectrophotometer supplied by Japanese company (Shimadzu) was used to record the optical absorbance and transmittance spectra of CdS: Cu thin films at wavelength range (400-1100) nm. Surface morphology of the films were studied by using (CSPM AA3000) Atomic Force icroscope(AFM) supply by Angstrom Company.X-ray diffraction (XRD) patterns of the CdS:Cu films which deposited on corning glass substrate were recorded by SHIMADZU XRD-6000 X-ray diffract meter ($\text{CuK}\alpha$ radiation $\lambda=0.154\text{nm}$) in 2θ range from 20° to 60° . The interplaner distanced d_{hkl} for different planes is measured using Bragg law [12]

$$2d \sin \theta = n \lambda \dots\dots\dots(1)$$

The grain size of the films were calculated using Scherrer formula [13] :

$$G.S = \frac{K \lambda}{\beta \cdot \cos(\theta)} \dots\dots\dots(2)$$

where, K : constant taken to be 0.94, β : is the f

ull width at half maximum (FWHM) in radian , λ : is the X-ray wavelength (1.5406\AA) and θ = Bragg's angle .

The thickness of prepared films was about 300 nm which was measured by Michelson interferometer. An optical transmittance and absorbance spectra were recorded, at room temperature, in the wavelength range 300-1100nm using OPTIMA SP-3000 UV-VIS spectrophotometer. The absorption coefficient (α) of pure and Cu-doped CdSnanocrystalline were calculated from the optical transmittance spectrum measurements using the formula[14]:

$$\alpha = \frac{1}{t} \ln \left(\frac{1}{T} \right) \dots\dots\dots(3)$$

where (t) is the thickness of thin films, and T is the transmittance intensity. The energy gap and optical constants were calculated as a function of different Cu concentrations.

3 RESULTS AND DISCUSSION

3.1 X-Ray Diffraction Analysis

The X-ray diffraction patterns of pure and doped CdS nanocrystalline with different doping ratio of Cu (0, 1,2,3 and 4%) deposited by CBD method on glass substrate with thickness (300) nm are shown in Figs. 1. The XRD patterns for all cases reveal polycrystalline in nature and have a good identical standard peaks for both hexagonal and cubic CdS with increasing Cu concentration. appears at 26.49° at Cu concentration (0&1% wt) while at Cu content increase to(2,3,4)%wt another peak appears at 30.8° corresponding to the reflection from (200) plane. Our results are agree with the results obtained by *Al-Hamdani N A and SalihA H [15]*. In addition we can also see from table (I) a decrease in dhkl with increasing Cu content i.e., slight shift in 2θ to higher value because the size of Cu ion (which have been inserted into lattice) is lesser than Cd ion (covalent radii for Cd=14.8 and for Cu= 1.38Å) [16].

The intense and sharp peaks in the XRD pattern reveal the good crystallinity of the thin films and confirm the stoichiometric nature of CdS:Cu thin films. The preferential orientation (002) in CdS:Cu thin films where x= 0 (CdS film) it was reported for thermal vacuum evaporated [17] - [18] - [19] while it was reported for chemical bathed [20].

Table II illustrates bragg's angles, inter planersspacing, relative intensities, miller indices, and latticeconstants of CdS:Cu thin films. The diffraction peaks for (002) are located at 26.44° and 30.8° Cu content (0, 1and2,3 4)%wt respectively.

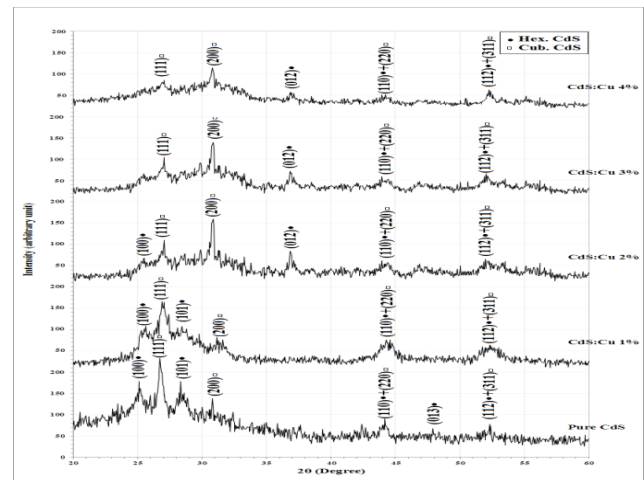


Fig. 1. X-ray diffraction patterns forCdS:Cu with different Cu ratio (0, 1, 2, 3 and 4%)

TABLE 1
STRUCTURAL PARAMETERS: INTER-PLANAR SPACING,
CRYSTALLINE SIZE OF DEPOSITED PURE AND DOPED
CDSNANOCRYSTALLINE AT DIFFERENT CU DOPING
RATIO (0, 1, 2, 3 and 4%)

Cu%	2θ (Deg.)	FWHM (Deg.)	d _{hkl} Exp.(Å)	d _{hkl} Std.(Å)	G.S (nm)	phase	hkl	card No.
0	24.9881	0.7111	3.5606	3.5808	11.448	Hex.CdS	(100)	96-900-8863
	26.4907	0.4562	3.3620	3.3544	17.899	Cub.CdS	(111)	96-101-1252
	28.1656	0.7097	3.1657	3.1632	11.546	Hex.CdS	(101)	96-900-8863
	30.7846	0.3553	2.9021	2.9050	23.202	Cub.CdS	(200)	96-101-1252
	43.8081	0.7110	2.0649	2.0674	12.048	Hex.CdS	(110)	96-900-8863
				2.0541		Cub.CdS	(220)	96-101-1252
	47.9301	0.6599	1.8965	1.9049	13.180	Hex.CdS	(013)	96-900-8863
	51.7974	0.7105	1.7636	1.7629	12.435	Hex.CdS	(112)	96-900-8863
1.7518				Cub.CdS		(311)	96-101-1252	
1	25.5067	0.8608	3.4894	3.5808	9.467	Hex.CdS	(100)	96-900-8863
	26.8867	0.7461	3.3134	3.3544	10.953	Cub.CdS	(111)	96-101-1252
	28.4935	0.5739	3.1120	3.1632	14.289	Hex.CdS	(101)	96-900-8863
	30.8708	0.8608	2.8942	2.9050	9.579	Cub.CdS	(200)	96-101-1252
	44.3902	1.2052	2.0391	2.0674	7.122	Hex.CdS	(110)	96-900-8863
				2.0541		Cub.CdS	(220)	96-101-1252
	51.9379	1.7217	1.7591	1.7629	5.135	Hex.CdS	(112)	96-900-8863
				1.7518		Cub.CdS	(311)	96-101-1252
2	25.5519	0.6313	3.4733	3.5808	12.910	Hex.CdS	(100)	96-900-8863
	27.0588	0.4591	3.2927	3.3544	17.806	Cub.CdS	(111)	96-101-1252
	30.8910	0.3443	2.9924	2.905	23.950	Cub.CdS	(200)	96-101-1252
	36.8723	0.6887	2.4357	2.4558	12.165	Hex.CdS	(012)	96-900-8863
	44.3902	1.1478	2.0391	2.0674	7.478	Hex.CdS	(110)	96-900-8863
				2.0541		Cub.CdS	(220)	96-101-1252
	51.9656	1.5495	1.7583	1.7629	5.706	Hex.CdS	(112)	96-900-8863
				1.7518		Cub.CdS	(311)	96-101-1252
3	27.0588	0.7461	3.2927	3.3544	10.957	Cub.CdS	(111)	96-101-1252
	30.9465	0.4591	2.8873	2.905	17.963	Cub.CdS	(200)	96-101-1252
	36.8149	0.7461	2.4394	2.4558	11.227	Hex.CdS	(012)	96-900-8863
	44.4181	1.1478	2.0379	2.0674	7.479	Hex.CdS	(110)	96-900-8863
				2.0541		Cub.CdS	(220)	96-101-1252
	52.0803	0.6887	1.7547	1.7629	12.844	Hex.CdS	(112)	96-900-8863
1.7518				Cub.CdS		(311)	96-101-1252	
4	27.0640	0.6887	3.2920	3.3544	11.870	Cub.CdS	(111)	96-101-1252
	30.9891	0.4591	2.8334	2.905	17.965	Cub.CdS	(200)	96-101-1252
	36.8723	0.5165	2.4357	2.4558	16.220	Hex.CdS	(012)	96-900-8863
	44.4210	0.6313	2.0378	2.0674	13.598	Hex.CdS	(110)	96-900-8863
				2.0541		Cub.CdS	(220)	96-101-1252
	52.2525	0.6313	1.7493	1.7629	14.022	Hex.CdS	(112)	96-900-8863
1.7518				Cub.CdS		(311)	96-101-1252	

Table (2) shows a decrement in lattice constants with increase Cu content for Hexagonal and cubic phases which have been observed in XRD patterns.

TABLE 2
LATTICE CONSTANTS FOR HEXAGONAL AND CUBIC PHASES: Cu LATTICE OBSERVED IN XRD PATTERNS

	doping %	Cubic		Hexagonal			
		a Std.(Å)	a Exp.(Å)	a Std.(Å)	a Exp.(Å)	c Std.(Å)	c Exp.(Å)
Cu	0	5.81000	5.8232	4.1348	4.1114	6.7490	6.9161
	1		5.7884		4.0292		6.8797
	2		5.7674		4.0106		5.8942
	3		5.7641		3.8021		5.8322
	4		5.7638		3.8013		5.5652

3.2 Atomic Force Microscopes (AFM) Analysis

Atomic force microscopy (AFM) is a non-invasive and convenient technique to study the morphological characteristics and surface roughness of semiconductor thin films and to observe microstructure of CdS:Cu nanocrystalline thin films. It is known that AFM is one of the most effective ways for the surface analysis due to its high resolution and powerful analysis software [21,22]. This technique offers digital images which allow quantitative measurements of surface features, such as root mean square roughness, R_q , or average roughness R_a , and the analysis of images from different perspectives, including three-dimensional simulation [23,24].

Figures (2 and 3) illustrates two and three dimensional AFM images for pure CdS and doped with different doping ratio of Cu (0, 1, 2, 3, and 4%) deposited by Chemical Bath Deposition on glass substrate. In addition it can be observed from AFM images that, nearly all the grains were pyramidal in shape. AFM parameters are indicated (average diameter, average roughness and root mean square roughness) for these samples have been shown in Table (3).

As observable, average grain size decreases with increasing Cu content while the root mean square roughness (R_q) and the average roughness (R_a) were found to increase with increasing the ratio of

Cu content, respectively. It is important to note that these obtained values are averaged and there is a statistical variation associated with them, which depends on the location of the measurements that are performed on the samples [24,25].

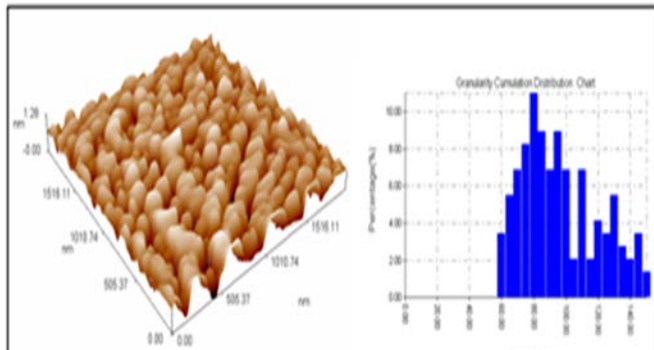


Fig. 2. Atomic force microscopy (AFM) images of CdS and CdS:Cu nanocrystalline thin films

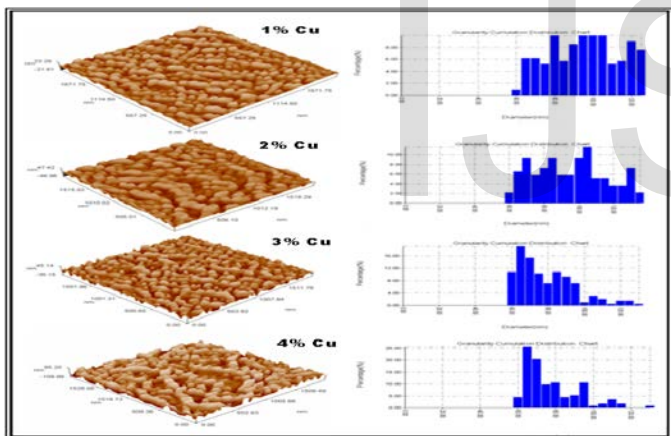


Fig. 3. AFM pictures and their granularity accumulation distribution for as deposited (CdS) nanocrystalline with different Cu content ratio (0, 1, 2, 3 and 4) %

TABLE 3
VARIATION OF SURFACE ROUGHNESS AND ROOT MEAN SQUARE FOR PURE CDS NANOCRYSTALLINE AND DOPED WITH CU

Doped type	Cu- content (x)	Average grain Size (nm)	The root mean square (Sq) (nm)	roughness average (Sa)(nm)
Cu	Pure CdS	93.73	0.239	0.193
	1	90.00	6	5.11
	2	92.75	11.4	9.62
	3	76.34	12.8	11.1
	4	75.56	37.2	32.3

3.3 Optical Properties

The optical properties of the films deposited on glass substrates are determined from the absorbance (A), and transmittance (T) measurements in the range (300–1100) nm are shown in Fig.(4). It was found that the transmittance of CdS:Cu films increases with the increasing in the wavelength. It is clear from the same figure that the transmittance decreases with increasing in Cu concentration which can be also deduced from the changing in the films' colour. Also it is clear that the transmittance of Cd:Cu thin films changes from $\approx 85\%$ to $\approx 35\%$ and this is consider a wide range which can be useful in different application like optical filters. In addition the variation of the transmittance of Cd:Cu thin films with the wavelength is very important because this variation will limit the transmitted wavelengths which play an important role in determination the category/type of the optical filters[26]

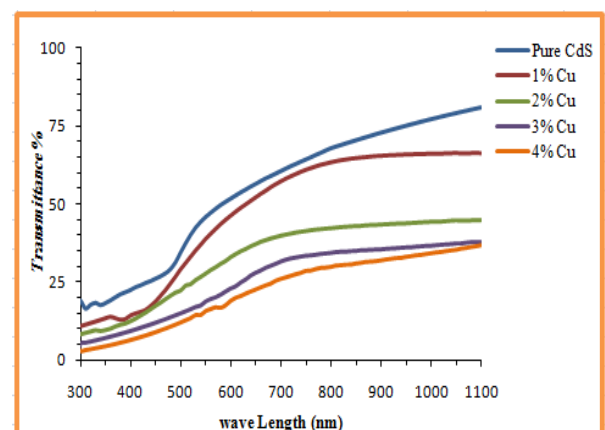


Fig. 4. Transmittance variation with the wavelength for pure and doped

Figure(5) illustrates the variation of absorption coefficient with wavelength for CdS:Cuthin films on glass substrate with different doping concentrations. It is clear that as the Cu concentration increases the absorption coefficient of CdS:Cu thin films is increased . This increasing in the absorbance is attributed to the copper atoms take Interfacial positions between atoms of cadmium sulfide and that increase the localized levels which results in an increase of the depth of donor levels associated with these vacancies and these levels will be available for the photons to be absorbed therefore the absorbance of CdS:Cu thin films will increase with increasing in Cu concentration . As well as from the same figure , it can be seen that the absorption edge shifts to the higher wavelengths corresponding to the red region as the Cu concentration increased. From this shifting in the absorption edge to the red region it can be deduced that the energy gap of CdS:Cu thin films will decrease with increasing in Cu concentration . Also the same figure shown the values of absorption coefficientincreases with increasing of Cu concentration and take the values($7 \times 10^4 \text{ cm}^{-1}$, $9 \times 10^4 \text{ cm}^{-1}$, $10 \times 10^4 \text{ cm}^{-1}$ and $12 \times 10^4 \text{ cm}^{-1}$ for Cu ratio equal (0 , 1 , 2,3 and 4) % wt respectively.

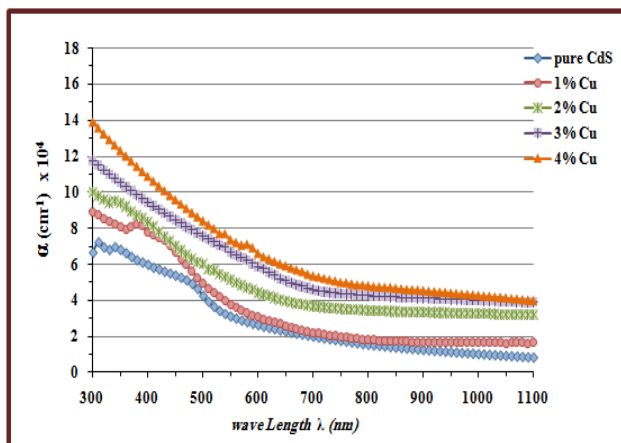


Fig. 5. Variation of absorbance coefficient with the wavelength for purenanocrystallineCdS and doped with Cu .

The optical energy gap values (E_g) for CdS:Cu thin films prepared by chemical deposition method have been determined from the region of

the high absorption at the fundamental absorption edgeof these films by using Tauc equation [15,27]:

$$\alpha h\nu = B \left(h\nu - E_g \right)^r \dots\dots\dots(4)$$

where $h\nu$ is the photon energy, E_g is the optical energy gap, B is a constant depends on the nature of the material (properties of its valence and conduction band) [28] and r : is a constant depends on the nature of the transition between the top of the valence band and bottom of the conduction band [29,30].

This equation is used to find the type of the optical transition by plotting the relations $(\alpha h\nu)^2$, $(\alpha h\nu)^{2/3}$, $(\alpha h\nu)^{1/2}$ and $(\alpha h\nu)^{1/3}$ versus photon energy ($h\nu$) and select the optimum linear part. It is found that the first relation yields linear dependence, which describes the allowed direct transition , then E_g was determined by the extrapolation of the portion at ($\alpha=0$) as shown in Fig.(6). It is clear that the optical energy gap for CdS:Cu thin films decreases and shifts towards the red region as the Se concentration in the films increased. This is attributed to the increasing the width of localized state with increasing of Cu which results increase of the depth of donor levels which in turn causing a reduction in the optical energy gap for CdS:Cuthin films[29] . The obtained values of the optical energy gap match well with the reported values of CdS [31]-[32]

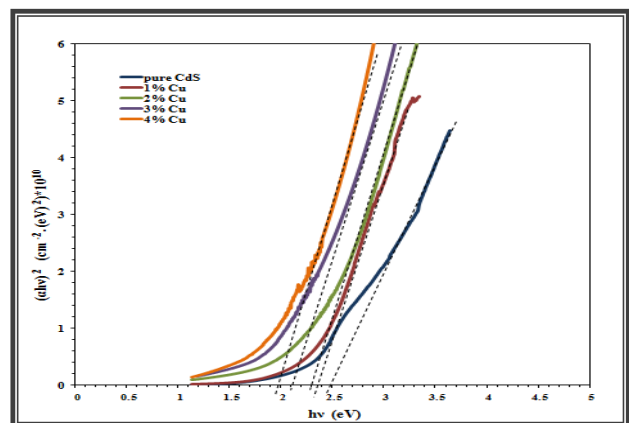


Fig. 6. The variation of $(\alpha h\nu)^2$ versus photon energy ($h\nu$) for pure and doped CdSnanocrystalline with Cu.

It is important to determine the optical constants of thin films such as refractive index (n), extinction coefficient (k), and the real (ϵ_r) and imaginary (ϵ_i) parts of dielectric constant.

The extinction coefficient (k_0) have been determined by using the following equation [33]:

$$k_0 = \frac{\alpha \lambda}{4\pi} \dots\dots\dots (5)$$

Where, α : is the absorption coefficient and λ : is the wavelength of the incident photon ..

It is clear from this equation that k_0 depends on α and has a similar behavior to α . Fig. (7) illustrates the variation of the extinction coefficient of CdS:Cu thin films with the wavelength for different ratio of Cu concentration . From this figure , it can be noted that k_0 varies slightly with the increasing in the wavelength corresponding to the reduction in the photons' energy and the increasing in the absorption coefficient. Then k_0 increases highly at the absorption edge region and this increasing is attributed to the increasing of the absorption coefficient due to the direct electronic transitions thereafter k_0 reaches to its maximum value at the high absorption region corresponding to the increment in the photons' energy and the increasing in the absorption coefficient with the decreasing in the wavelength . In addition , it is clear from this figure that

with the increasing in the Cu concentration the extinction coefficient k_0 increases . This is attributed to the increasing in the absorption coefficient due to the increasing of the depth of donor levels and these levels will be available for the photons to be absorbed causing an increment in the absorbance and leads to increase in the absorption coefficient .Therefore k_0 will increase with the increasing in the Cu concentration since it has a similar behavior to α and depends on it .

Fig. 7. Extinction coefficient versus wavelength for pure and doped CdSnanocrystalline with Cu.

The refractive index (n_0) of pure CdSnanocrystalline thin films and doped with Cu was estimated from the reflectance (R) data using the relation.[33]:

$$n = \sqrt{\frac{4R}{(1-R)^2} - k^2} - \frac{R+1}{R-1} \dots\dots\dots (6)$$

The variation of the refractive index as a function of the wavelength for CdS:Cu thin films is illustrated in Fig. (8). It is clear from this figure that the refractive index decreases with the increasing in the wavelength of the incident photon . Also it can be observed , that the refractive index of CdS:Cu thin films increases with the increasing in the Cu concentration at the spectrum region (500-1100)nm . This increasing is attributed to the decreasing in the grain size of the films with the increasing in the Cu concentration which interns causing an increment in the surface area of the films which in turns reduces the speed of light in the material of the thin film and then leads to an increasing in the refractive index .

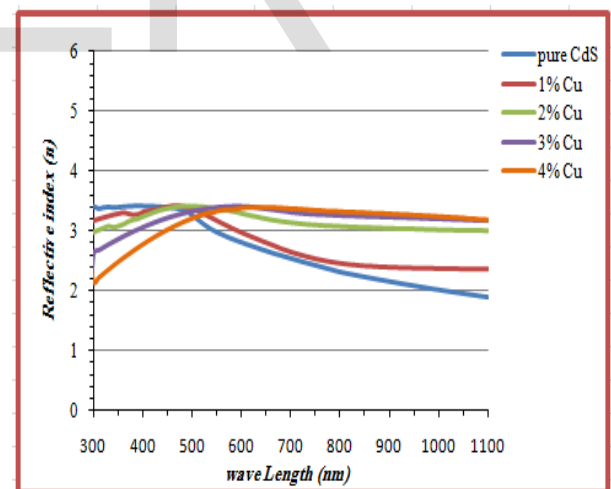


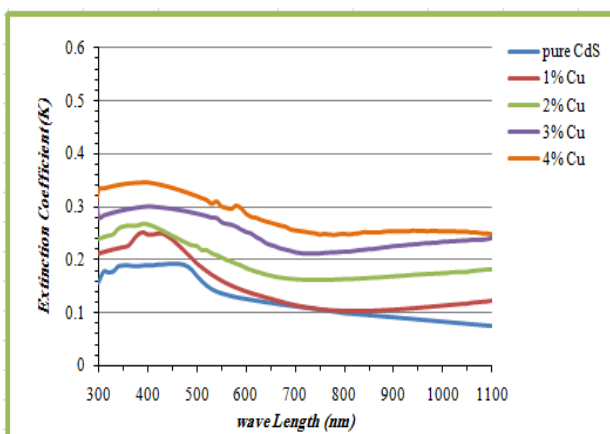
Fig. 8. The variation of refractive index with the wavelength for CdS and CdS:Cu nanocrystalline thin films

The real and imaginary parts of dielectric constant were evaluated using the formulas.[34] .

$$\epsilon_r = n^2 - k^2 \dots\dots\dots (7)$$

$$\epsilon_i = 2nk \dots\dots\dots (8)$$

The variation of the real and imaginary parts of the dielectric constants values versus wavelength have been shown in figures (9 and 10) for pure



CdSnanocrystalline thin films and doped with Cuon glass substrate. it can be observed , that the values of ϵ_r and ϵ_i of CdS:Cu thin films increases with the increasing in the Cu concentration .

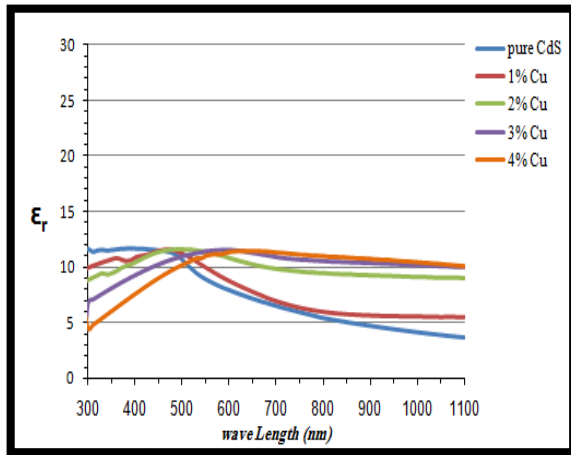


Fig. 9. The variation of ϵ_r with the wave length for pure and doped CdSnanocrystalline with Cu

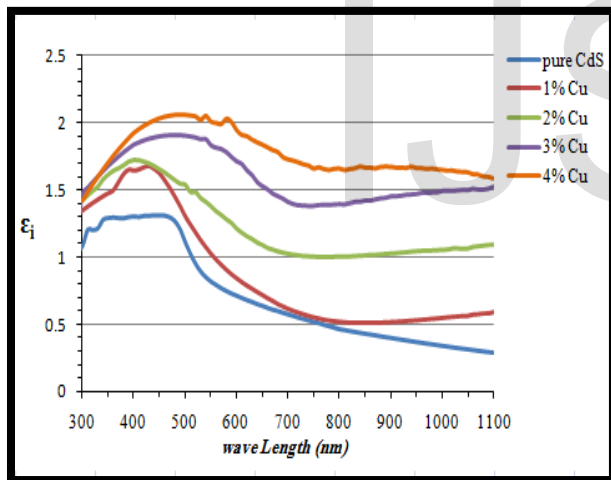


Fig. 10. The variation of ϵ_i with the wave length for pure and doped CdSnanocrystalline with Cu.

Table (4) shows the optical constants for deposited pure and Cu doped CdSnanocrystalline on glass with different doping concentrations (0, 1, 2, 3 and 4%) at $\lambda = 550$ nm and the optical energy gap values for these prepared samples. This Table illustrates that the values of α , k , n , ϵ_r , ϵ_i in general increase with cumulative Cu dopant concentrations, whereas the behavior of T is opposite i.e., decrease with increasing Cu doping concentrations.

TABLE 4
THE OPTICAL PARAMATARS AT $\lambda=550$ nm and E_g FPR PURE AND DOPED CDSNANOCRYSTALLINE AT DIFFERENT CU DOPING CONCENTRATIONS.

Cu %	T%	α (cm^{-1})	K	n	ϵ_r	ϵ_i	$E_g(eV)$
0	45.762	26061.9	0.114125	2.982474	8.882127	0.680747	2.50
1	38.77966	31581.5	0.138295	3.164997	9.998078	0.875405	2.35
2	27.64	42876.1	0.188	3.377	11.37	1.268	2.30
3	18.8545	55624	0.243576	3.397979	11.48693	1.655334	2.10
4	15.86524	61379	0.268778	3.34857	11.14068	1.800041	1.95

4 CONCLUSIONS

- Chemical bath deposition method technique can be successfully employed for the deposition of uniform morphologist and nanocrystallineCdS:Cutthin films with hexagonal phase at R.T
- XRD indicates that all CdS:Cunanocrystalline have polycrystalline structure and have booth hexagonal and cubic phases and increase the cubic phase with increasing Cu ratio.
- The results of AFM for the CdS:Cunanocrystalline films, observed the smooth surface texture with lower Cu- concentration . The root mean square and Surface roughness increases with increasing copper content .
- Optical studied indicates that CdS:Cutthin films exhibit direct band gap which is strongly depends on the Cu concentration almost cover the entire visible spectral that makes these films are suitable for optoelectronic devices especially for solar cell.

REFERENCES

- [1] KovtyukhovaN I,BuzanevaE V, WaraksaC C and MalloukT E 2000*Materials Science and Engineering B*, Vol. 69-70 .
- [2] Aguilar-H J, Sastre-H J, Ximello- QN and Mendoza-P R 2006*Thin Solid Films*, Vol. 511-512 .
- [3] IsahK U 2013 *Materials Sciences and Applications*, Scientific research 4, 287-292 .
- [4] AwodugbaAO and AdedokunO2011*Science and Technology*, Volume 12. Number 2.
- [5] Godovski D Y 1995 *Adv. Polym. Sci.* 119 pp. 79-122.

ISSN 2229-5518

[6] Herron N, Wang Y and Eckert H 1990 *J. Am. cChem. So.* 112 pp. 1322-1326.

[7] KarS and Chaudhuri S 2006 *Met. Org. Nano-Metal Chem.* 36 - 289–312.

[8] Xu Y N and Ching W Y 1993 *Physical Review B* 484335-4351.

[9] Skinner B 1961 *American Mineralogist* 46. 1399-1411.

[10] Quiebras J X, Puente G C, Hernandez J A, Rodriguez G and Carbajal Readigos A 2004 *Sol. Energ. Mater. Sol Cells* 82 263.

[11] Neamen D A 2003 *Semiconductor Physics and Devices Basic Principles* (Third Edition University of new Mexico) Pubh5hedby McGraw-Hill.

[12] Attila 1999 *Fundamentals of the Physics of Solids* Vol. I Structure and Dynamics Translated (1999) Piroth 242,261.

[13] Konczos G, Barsony I and Deak P 1998 *Introduction to materials science and technology* (Textbook of Technical University Budapest for PhD Students in Physics).

[14] Rizwan Z, Zakaria A, Ghazali M and Jafari A 2011 *Int. J. Mol. Sci.* 12 1293.

[15] Al-Hamdani N A and Salih A H 2012 *Diyala Journal for Pure Sciences* Vol. 8 No. 3.

[16] Sanderson's R T 1960 *Chemical periodicity* (Reinhold).

[17] A. Ashour, The physical characteristics of Cu₂S/CdS thin-films solar cell, *Journal of Optoelectronics and Advanced Materials* Vol. 8, No. 4, August (2006), p. 1447 – 1451.

[18] L. Ion, I. Enculescu, S. Iftimie, V. Ghenescu, C. Tazlaoanu, C. Besleaga, T. L. Mitran, V. A. Antohe, M. M. Gugiu and S. Antohe, Effect of proton irradiation on the spectral performance of photovoltaic cells based on CdS/CdTe thin films, *Chalcogenide Letters* Vol. 7, No. 8, August (2010), p. 521-530.

[19] Z.R. Khan, M. Zulfequar and M.S. Khan, Effect of thickness on structural and optical properties of thermally evaporated cadmium sulfide polycrystalline thin films, *Chalcogenide Letters* Vol. 7 No. 6, June (2010), p. 431-438.

[20] R. Mendoza-Pérez, G. Santana-Rodríguez, J. Sastre-Hernández, A. Morales-Acevedo, A. Arias-Carbajal, O. Vigil-Galan, J.C. Alonso and G. Contreras-Puente, Effects of thiourea concentration on CdS thin films grown by chemical bath deposition for CdTe solar cells, *Thin Solid Films*, Vol. 480-481, (2005), p. 173–176.

[21] Amirul M, Yunus S M, Talib Z A and Yunus W M 2011 *Journal of Chemical Engineering and Materials Science* Vol. 2, No. 7, p. 103-109.

[22] Abbas N K, Naji I S and Abdulmajeed A A 2012 *International Review of Physics* (I.R.E.PHY.) Vol. 6 N. 3 ISSN 1971-680X.

[23] Nabiyouni I G, Sahraei R, Toghiani M and Majles M H 2011 *Rev. Adv. Mater. Sci.* 27 52-57.

[24] Abbas N K, Al-Rasoul K T and Shana Z J 2013 *International Journal of Electrochemical Science* Vol. 8.

[25] A. Martynes, C. Guillen and J. Herrero // *Appl. Surf. Sci.* 140 (1999) 182.

[26] Jafari A and Zakaria A 2011 *UMTAS Technology and Innovation Towards a Better Tomorrow* 246-250.

[27] Moreno O P, Lima-Lima H, Juárez-Díaz G and Rebollo-Plata B 2006 *Journal of The Electrochemical Society* 153(10)G926-G930.

[28] S. O. Kasap, "Principle of electronic materials and devices", (Snded, McGraw-Hill, New York, 2002).

[29] Abbas T A and Ahmad J M 2013 *Journal of Electron Devices* Vol. 17, pp. 1413-1416.

[30] Z.R. Khan, M. Zulfequar and M.S. Khan, Effect of thickness on structural and optical properties of thermally evaporated cadmium sulfide polycrystalline thin films, *Chalcogenide Letters* Vol. 7, No. 6, June (2010), p. 431-438.

[31] Yadav A. A. and Masumdar E. U., Optical and electrical transport properties of spray deposited CdS_{1-x}Se_x thin films, *Journal of Alloys and Compounds* Vol. 505, (2010), p. 787-792.

[32] Rusu M. Rumberg A., Schuler S., Nishiwaki R., Wu'rz R., Babu S. M., Dziedzina M., Kelch C., Siebentritt S., Klenk R., Th. Schedel-Niedrig, M. Ch. Lux-Steiner, Optimization of the CBD CdS deposition parameters for ZnO/CdS/CuGaSe₂/Mo solar cells, *Journal of Physics and Chemistry of Solids* Vol. 64, (2003), p. 1849–1853.

[33] Aksoy S, Caglar Y, Ilıcın S and Caglar M 2010 *Optica Applicata*, V. XL, N.1.

[34] Kazmerski L 1980 "Polycrystalline and Amorphous Thin Films and Devices" Academic Press.